

1 **Classification:**

2 **Biological Sciences: Cell Biology; Developmental Biology; Genetics.**

3

4 **DNA methylation is indispensable for leukemia inhibitory factor dependent**
5 **embryonic stem cells reprogramming**

6 Baojiang Wu^{a,b,j,1}, Yunxia Li^{a,b,j,1}, Bojiang Li^{c,1}, Baojing Zhang^{a,b,1}, Yanqiu Wang^{a,b}, Lin Li^{d,e},
7 Junpeng Gao^e, Yuting Fu^{a,b}, Shudong Li^f, Chen Chen^{a,b}, M. Azim Surani^g, Fuchou Tang^{e,h,i},
8 Xihe Li^{a,b,j,2}, and Siqin Bao^{a,b,2}

9

10 ^aThe State Key Laboratory of Reproductive Regulation and Breeding of Grassland Livestock,
11 Inner Mongolia University, Hohhot, 010070, China

12 ^bResearch Center for Animal Genetic Resources of Mongolia Plateau, College of Life
13 Sciences, Inner Mongolia University, Hohhot, 010070, China

14 ^cCollege of Animal Science and Veterinary Medicine, Shenyang Agricultural University,
15 Shenyang, 110866 China

16 ^dGuangdong Provincial Key Laboratory of Proteomics, Department of Pathophysiology,
17 School of Basic Medical Sciences, Southern Medical University, Guangzhou 510515, China

18 ^eBeijing Advanced Innovation Center for Genomics and Biomedical Pioneering Innovation
19 Center, College of Life Sciences, Peking University, Beijing 100871, China

20 ^fCancer Research UK and Medical Research Council Oxford Institute for Radiation Oncology,
21 Department of Oncology, University of Oxford, Oxford OX3 7DQ, UK

22 ^gWellcome Trust Cancer Research UK Gurdon Institute, Tennis Court Road, University of
23 Cambridge, Cambridge, CB2 1QN UK

24 ^hPeking–Tsinghua Center for Life Sciences, Peking University, Beijing, 100871, China

25 ⁱMinistry of Education Key Laboratory of Cell Proliferation and Differentiation, Beijing,
26 100871, China

27 ^jInner Mongolia Saikexing Institute of Breeding and Reproductive Biotechnology in Domestic
28 Animal, Huhhot, 011517, China

29 ¹B.W., Y.L., B.L. and B.Z. contributed equally to this work.

30 ²To whom correspondence may be addressed. Email: lixh@life.imu.edu.cn or
31 baosq@life.imu.edu.cn

32

33 **Keywords:** Embryonic stem cells; Leukemia inhibitory factor; Reprogramming; Epigenetic;
34 Genomic imprinting; DNA methylation

35 **Abstract**

36 **Naïve pluripotency can be maintained by the 2i/LIF supplements (CHIR99021,**
37 **PD0325901 and LIF), which primarily affect canonical WNT, FGF/ERK, and**
38 **JAK/STAT3 signaling. However, whether one of these tripartite supplements alone is**
39 **sufficient to maintain naïve self-renewal remain unclear. Here we show that LIF alone is**
40 **sufficient to induce reprogramming of 2i/LIF cultured ESCs (2i/L-ESCs) to ESCs with**
41 **hypermethylated state (L-ESCs). *In vitro*, upon withdrawal of 2i, 2i/L-ESCs overcome**
42 **the epigenetic barrier and DNA hypermethylated, which accompanies transcriptional**
43 **changes and subsequent establishment of epigenetic memory. Global transcriptome**
44 **features also show that L-ESCs are close to 2i/L-ESCs and in a stable state between**
45 **naïve and primed pluripotency. Notably, our results demonstrate that DNA methylation**
46 **was indispensable for LIF-dependent mouse ESCs reprogramming and self-renew.**
47 **LIF-dependent ESCs reprogramming efficiency is significantly increased in serum**
48 **treatment and reduced in *Dnmt3a* or *Dnmt3l* knockout ESCs. Importantly, unlike**
49 **epiblast and EpiSCs, L-ESCs contribute to somatic tissues and germ cells in chimaeras.**
50 **Such simple culture system of ESCs is more conducive to clarify the molecular**
51 **mechanism of ESCs *in vitro* culture.**

52

53 **Significance**

54 Embryonic stem cell (ESCs) exhibit naïve pluripotency which reflects their ability to
55 contribute to all embryonic lineages upon injection into blastocyst. ESCs were originally
56 derived by co-culture with feeder cells and fetal calf serum. In this manuscript, we took a

57 detailed approach to dissect the roles of LIF alone in ESC reprogramming of 2i/LIF cultured
58 ESCs (2i/L-ESCs). Here, for the first time, we derived stable hypermethylated pluripotent
59 ESCs under culture of LIF alone (L-ESCs). We further assessed L-ESCs properties both in
60 vitro and in vivo, and provide molecular insights to the mechanism which allows LIF alone to
61 maintain pluripotency and a hypermethylated state. We believe these findings are novel and
62 valuable for future ESCs study.

63

64 **Introduction**

65 Mouse embryonic stem cells (ESCs) are isolated from the inner cell mass of the
66 pre-implantation embryos (1, 2). Since pluripotent mouse embryonic stem cells were first
67 established four decades ago, various culture systems of ESCs have been developed including
68 initially, using feeder/serum/cytokines, then feeder/serum/Leukemia inhibitory factor (LIF)
69 or Bone morphogenetic protein 4 (BMP4) (3-5), and more recently using 2i/LIF (two
70 inhibitors CHIR99021, PD0325901 and LIF) (6). It is generally believed that the optimal
71 culture condition for ground state ESCs comprises three additive 2i/LIF supplements which
72 affect canonical WNT, FGF/ERK, and JAK/STAT3 signals respectively (7). It has been
73 reported that combination of any two of these tripartite supplements was sufficient to maintain
74 naïve self-renewal of ESCs (8). However, whether any one of the tripartite supplements plays
75 a critical role with unique signalling targets for ESCs pluripotency and self-renewal remains
76 unanswered.

77

78 LIF is the most pleiotropic member of the interleukin-6 family of cytokines, and utilizes a

79 receptor that consists of the LIF receptor B and gp130 (7). LIF is able to activate three
80 intracellular signaling pathway: the JAK/STAT pathway, the PI3K/AKT pathway, and the SH2
81 domain-containing tyrosine phosphatase/MAPK pathway. LIF has antagonistic effects in
82 different cell types including stimulating or inhibiting cell proliferation, differentiation and
83 survival. Since LIF was detected in extract from feeder cells and has been used for most mice
84 ESCs medium, it has been fully demonstrated to be an important supplement for ESCs
85 self-renewal and pluripotency (4-6, 9-12). Nevertheless, essential LIF/STAT3 functions can be
86 compensated by activation of canonical WNT signaling and inhibition of FGF/ERK in the
87 established culture system for self-renewal of ESCs (7). However, the consequences
88 LIF/STAT3 signaling alone and precise regulatory mechanisms for ESCs self-renew have
89 remained largely elusive.

90

91 Mouse ESCs cultured in different culture conditions exhibit distinct DNA methylation
92 patterns. The 2i/LIF cultured ESCs (2i/L-ESCs) are globally DNA hypomethylated, whereas
93 ESCs are grown in classical medium containing feeders, serum and LIF (S/L-ESCs) show
94 global DNA hypermethylation (13, 14). Additionally, DNA methylation levels were shown to
95 be reversible between S/L-ESCs and 2i/L-ESCs (13). Recent research reported prolonged
96 MEK1/2 suppression impairs the epigenetic and genomic integrity as well as the
97 developmental potential of ESCs, in part through the downregulation of DNA methylation (15,
98 16). This suggests that DNA methylation plays an important role in ESCs and normal
99 development. We also showed that hypermethylation is a key point for expanded pluripotency
100 of ESCs in chemical defined medium (17).

101

102 The combination of 2i supports the self-renewal of ESCs in serum-free culture without LIF,
103 however, addition of LIF in 2i-culture condition further promoted self-renewal of ESCs,
104 suggesting the synergistic effect of 2i and LIF (6). PD0325901 suppresses the differentiation
105 of ESCs but does not support proliferation (6, 18). CHIR99021 is highly specific to GSK3
106 and it alone is not sufficient to support the self-renewal of ESCs in serum-free culture (6). In
107 this study, we focus on the JAK/STAT3 signaling and show that LIF alone is able to support
108 mouse embryonic stem cells self-renew and pluripotency as well as developmental potency.
109 Our data also suggest that DNA methylation is indispensable for LIF dependent mouse ESCs
110 reprogramming and self-renew. The detailed analysis of LIF alone dependent mouse ESCs
111 reprogramming provides mechanistic insight into global DNA (de)methylation and also
112 provides a rich resource for future studies on ESCs *in vitro* culture.

113

114 **Results**

115 **LIF alone supports ESCs self-renew and pluripotency in chemically defined** 116 **media**

117 Serum plus LIF (S/L) medium and 2i plus LIF (2i/LIF) medium (based N2B27) are two
118 typical ESCs culture media. In particular, LIF was found in almost all mice ESCs culture
119 media *in vitro*. Therefore, we sought to determine whether LIF alone is capable of driving
120 continuous cycles of self-renew of ESCs in the absence of serum and 2i medium. In here, we
121 used six Oct4-ΔPE-GFP (GOF/GFP, mixed background of MF1, 129/sv, and C57BL/6J
122 strains) ×129/sv F1 mice (19) ESCs lines (W1, W2, W4, W5, W6 and SQ3.3), which were

123 directly derived in 2i/L medium (passages 15-20) and then switched to chemically defined
124 LIF (1000 IU/ml) medium based on N2B27 (L-medium) (Fig. 1A and *SI Appendix*, Fig. S1A).
125 Initially ESCs showed signs of differentiation, such as flattening of colonies and reduction of
126 GOF/GFP positive (GOF/GFP⁺) for pluripotency-related transcription factors *Oct4* (Fig. 1B).
127 However, in passages 3-5, some GOF/GFP⁺ colonies similar to those in undifferentiated ESCs,
128 began to survive during LIF dependent ESCs reprogramming (Fig. 1B). Here we designated
129 these LIF-dependent GOF/GFP⁺ ESCs in chemically defined medium as L-ESCs. GOF/GFP⁺
130 colonies increased gradually with further passages (Fig. 1B).

131

132 Next, we performed fluorescence-activated cell sorting (FACS) on multiple L-ESCs lines and
133 the GOF/GFP⁺ L-ESCs were cultured in L-medium. The percentage of GOF/GFP⁺ L-ESCs
134 (passages, p14-p42) ranged from 56% to 99% in several ESCs line (*SI Appendix*, Fig. S1B).
135 After two or more repeated FACS for each L-ESCs line (*SI Appendix*, Fig. S1B), GOF/GFP⁺
136 L-ESCs reached nearly 98% purity, which was similar to the control 2i/L-ESCs (*SI Appendix*,
137 Fig. S1B). These data indicate that LIF alone can maintain FACS-purified GOF/GFP⁺ L-ESCs
138 in undifferentiated pluripotent state (Fig. 1B and *SI Appendix*, Fig. S1B) with stable growth
139 over 40 passages (*SI Appendix*, Fig. S1C), and high alkaline phosphatase (AP) activity (*SI*
140 *Appendix*, Fig. S1D). The established L-ESCs lines have normal karyotype (Fig. 1C) and
141 express pluripotent markers OCT4, SOX2, and NANOG, confirmed by immunofluorescence
142 (Fig. 1D). In mouse ESCs, < 1% of cells exhibit some features of 2-cell (2C) embryos, such
143 as the expression of 2C specific transcripts (20, 21). Interestingly, L-ESCs also retained 2C
144 features, such as ZSCAN4 and MERVL activities demonstrated by immunostaining (Fig *SI*

145 *Appendix*, Fig. S1E). It has been reported that both X chromosomes are active in female naive
146 ESCs cells (22, 23), concurrent with this, our immunostaining showed no H3K27me3 foci in
147 female L-ESCs, suggesting that both X chromosomes are activated (*SI Appendix*, Fig. S1F).
148 These results suggest that L-ESCs possess most of the characteristics of 2i/L-ESCs.

149

150 For a further stringent test of the pluripotency of L-ESCs, we examined the ability of clone
151 formation from single cell level. We observed that L-ESCs could form single cell derived
152 colonies in chemically defined LIF alone condition with high efficiency, comparable to those
153 from 2i/L-ESCs (Fig. 1E). Furthermore, to examine how essential LIF is in maintaining
154 L-ESCs, we withdrew LIF and then added JAK inhibitor I, and observed significantly
155 impaired propagation of L-ESCs with rapid differentiation (Fig. 1F). However, LIF
156 withdrawal and JAK inhibitor addition did not affect the self-renewal of 2i/L-ESCs until
157 passages 10 (Fig. 1G). Taken together, our results suggest that LIF is an important and
158 essential regulator in the maintenance of L-ESCs. In contrast to the previous notion that LIF
159 and 2i were both indispensable for ESCs self-renewal, and established unique ground state of
160 ESCs, in this study we showed that LIF alone is capable to support ESCs for self-renewal and
161 proliferation over passage 40.

162

163 **Global transcriptome features of L-ESCs**

164 To examine whether L-ESCs have distinct molecular features, we carried out RNA
165 sequencing (RNA-seq) on L-ESCs, 2i/L-ESCs, S/L-ESCs and EpiSCs. Unsupervised
166 hierarchical clustering (UHC) and principal component analysis (PCA) showed L-ESCs close

167 to 2i/L-ESCs (Fig. 2A and B) and appeared to be at an intermediate state between naïve ESCs
168 and primed EpiSCs (Fig. 2A). Comparing L-ESCs and 2i/L-ESCs, L-ESCs differentially
169 expressed genes were related to embryonic morphogenesis, cellular lipid metabolic processes,
170 pattern specification processes, embryonic organ morphogenesis and DNA hypermethylation.
171 Whereas 2i/L-ESCs differentially expressed genes were related to stem cell development,
172 stem cell proliferation, WNT-protein binding, gamete generation and meiotic cell cycle phase
173 (Fig. 2C). This shows L-ESCs display distinct molecular features for pluripotency.
174 Interestingly, Compared with L-ESCs, 2i/L-ESCs, S/L-ESCs and EpiSCs, among
175 differentially expressed genes (24), 3,347 genes (profile 7) were significantly high expressed
176 in L-ESCs and 2i/L-ESCs compared with S/L-ESCs and EpiSCs (Fig. 2D). Notably, a total of
177 1,621 genes (profile 2) were significantly upregulated in 2i/L-ESCs, compared with L-ESCs,
178 S/L-ESCs and EpiSCs (Fig. 2D). These RNA-seq analyses suggest that L-ESCs are in a stable
179 state between naïve and primed pluripotency.

180

181 **L-ESCs exhibit DNA hypermethylation and reserve genomic imprints**

182 ESCs cultured in 2i/LIF or in LIF plus serum supplemented media represent two states of
183 pluripotency of ESCs. Despite their similarities in pluripotency, 2i/L and S/L-ESCs rely on
184 different signaling pathways and display strong differences in transcriptional and epigenetic
185 landscapes (25-27). Here, we asked whether there are different epigenetic marks among
186 L-ESCs, 2i/L-ESCs and S/L-ESCs. Whole-genome bisulfite sequencing (WGBS) was
187 performed and DNA methylation profiling of L-ESCs with 2i/L-ESCs and S/L-ESCs was
188 compared. The levels of DNA methylation in L-ESCs (median CpG methylation of ~80%)

189 were comparable to S/L-ESCs (median ~90%) and higher than 2i/L-ESCs (median ~30%)
190 (Fig. 3A). This DNA methylation occurs across most methylated regions including intragenic,
191 intergenic, exon, intron, short and long interspersed nuclear elements (SINEs and LINEs,
192 respectively) and long terminal repeats (LTRs) (*SI Appendix*, Fig. S2A). Additionally,
193 expression of DNA methylation associated genes was assessed using qPCR. As expected,
194 DNA methyltransferases *Dnmt3a* and *Dnmt3l* was significantly upregulated in GOF/GFP
195 positive L-ESCs compared with GOF/GFP negative cells from the L-ESCs reprogramming
196 process (*SI Appendix*, Fig. S2B). Moreover, the transcriptional level of genes known to
197 influence DNA methylation levels, such as *Prdm14* and *Nanog* were significantly
198 downregulated in L-ESCs (*SI Appendix*, Fig. S2B).

199

200 Next, we examined the dynamic changes of DNMT3A level in the process of L-ESCs
201 reprogramming. Interestingly, the protein level of DNMT3A was high in early reprogramming
202 stage (day 5) GOF/GFP positive L-ESCs (Fig. 3B and C). Upon withdrawal of PD0325901
203 and CHIR99021, heterogeneous expression of DNMT3A was detected in nuclei of L-ESCs
204 reprogramming at day 5, and in long-term culture the DNMT3A protein level was
205 significantly increased in p27 stage L-ESCs (Fig. 3B), consistent with the higher methylation
206 in L-ESCs. These data is also consistent with the notion that PD0325901 promotes
207 downregulation of DNA methylation (15, 16). The results showed DNMT3A is important
208 factor to regulate DNA methylation in L-ESCs which possess hypermethylation state.

209

210 Proper genomic imprinting is essential for embryonic development (28, 29). We further

211 performed genomic imprinting analysis on L-ESCs, S/L-ESCs and 2i/L-ESCs. Notably,
212 compared with 2i/L-ESCs, the DNA methylation levels at imprinting control regions (ICRs)
213 were markedly higher in L-ESCs and were similar to S/L-ESCs (Fig. 3D). Collectively, we
214 conclude that L-ESCs exhibited global genomic hypermethylation and reserved genomic
215 methylation in the majority of imprinting control regions.

216

217 **Serum treatment increase the efficiency of LIF-dependent ESCs** 218 **reprogramming**

219 Since the S/L-ESCs possess high levels of DNA methylation (25), we next asked if serum
220 treatment (prior to reprogramming of L-ESCs) may enhance the DNA methylation and then
221 increase the efficiency of LIF dependent L-ESCs reprogramming. We switched 2i/L-ESCs to
222 S/L-medium for five days of induction, then S/L-ESCs were cultured in LIF only (L-medium)
223 to assess the LIF dependent L-ESCs reprogramming. Our result indicates that S/L induction
224 for 5 days significantly increased the number of AP⁺ colonies compared with 2i/L-ESCs (Fig.
225 4A and *SI Appendix*, Fig. S3A). Consistent with this, 1×10^5 cells were seeded into 24-well
226 cell culture plate in L-medium, the number of GOF/GFP⁺ colonies obtained from S/L
227 induction group compared with 2i/L-ESCs was drastically increased (Fig. 4B). To confirm
228 this, flow cytometry analysis showed that the percentage of GOF/GFP⁺ cells in the S/L
229 induction group was also increased compared with 2i/L-ESCs (Fig. 4C). Furthermore, we
230 tested this reprogramming process of ASCs in LIF alone medium using our previously
231 published hypermethylated ASCs (17, 30) and showed that ASCs can also be efficiently
232 reprogrammed into LIF-dependent ESCs using L-medium (*SI Appendix*, Fig. S3B and C).

233 **DNA methylation is indispensable for L-ESCs self-renewal**

234 Next, we asked whether DNA methylation is critical for this reprogramming, and investigated
235 roles of different DNA methyltransferase in the early reprogramming processes. We separated
236 GOF/GFP⁺ and GOF/GFP⁻ L-ESCs from early reprogramming processes by FACS. As
237 expected, *Dnmt3a* and *Dnmt3l* expression levels in GOF/GFP⁺ L-ESCs were significantly
238 higher than in GOF/GFP⁻ L-ESCs (*SI Appendix*, Fig. S2B), as well as DNMT3A protein level
239 (Fig. 3C). Interestingly, we also found higher expression level of H3K36me3 in GOF/GFP⁺
240 early reprogramming stage (day 5) L-ESCs (Fig. 4D). This result is consistent with recent
241 reports of H3K36me3 as a guard for the DNA methylation process (31).

242

243 To unequivocally demonstrate whether stable L-ESCs self-renewal depends on DNA
244 methylation, we next examined the role of DNA methyltransferases (DNMTs) on the
245 regulating L-ESCs self-renewal processes by the DNMT inhibitor 5-aza-2'-deoxycytidine
246 (5-Aza). 5-Aza has been widely used as a DNA methylation inhibitor to experimentally
247 induce gene expression and cellular differentiation (32, 33). We cultured 2i/L-ESCs and
248 L-ESCs in their respective medium with 5-Aza and observed morphological changes of both
249 2i/L-ESCs and L-ESCs. 5-Aza treated 2i/L-ESCs retained typical dome-shaped clonal
250 morphology and were able to stably propagate at least ten passages (Fig. 5A and *SI Appendix*,
251 Fig. S4A). In addition, there were slight changes in the expression level of pluripotent genes
252 (including *Nanog*, *Sox2* and *Prdm14*) between 5-Aza treated 2i/L-ESCs and untreated
253 2i/L-ESCs (*SI Appendix*, Fig. S3B). However, 5-Aza treated L-ESCs failed to maintain its
254 self-renewal. There were few GOF/GFP⁺ L-ESCs which survived after seven days upon

255 5-Aza treatment and cells underwent apoptosis eventually (Fig. 5B). These data indicate that
256 L-ESCs are differentially sensitive to inhibition of DNA methyltransferase by 5-Aza
257 compared with 2i/L-ESCs.

258

259 To further investigate the important role of DNA methylation on LIF-dependent ESCs
260 reprogramming processes, we used *Dnmt3l* knockout ESCs (*Dnmt3l*^{-/-}-ESCs) which were
261 cultured in S/L medium (Fig. 5C) and generated *Dnmt3a* knockout ESCs line
262 (*Dnmt3a*^{-/-}-ESCs) which were cultured in ABC/L medium (Fig. 5D and E) (17) and then
263 switched to chemically defined LIF medium. As expected, both *Dnmt3l* and *Dnmt3a* knockout
264 cells significantly reduced the efficiency of LIF-dependent ESCs reprogramming (Fig. 5C and
265 F). Whereas wild type ESCs and ESCs derived L-ESCs displayed normal self-renew and
266 proliferation, the proliferation of *Dnmt3l*^{-/-} and *Dnmt3a*^{-/-} L-ESCs decreased dramatically (Fig.
267 5C and F; *SI Appendix*, Fig. S4A and C). Taken together, our data demonstrate that DNA
268 hypermethylation promotes the induction of LIF-dependent ESCs reprogramming.

269

270 ***In vitro* and *in vivo* differentiation ability of L-ESCs**

271 An important criterion for pluripotent ESCs is the ability to differentiate *in vitro* and *in vivo*
272 (34). Upon 2i and LIF withdrawal, pluripotent ESCs differentiate into three germ layers,
273 mesoderm, endoderm, and ectoderm (35). We cultured 2i/L-ESCs and L-ESCs in N2B27
274 basic medium only, without 2i/L and LIF. In these culture conditions, the ESCs differentiated.
275 After 3-day and 6-day differentiation, we performed quantitative qPCR analysis and
276 immunostaining. Interestingly, after 3-day differentiation, the expression level of all

277 mesoderm, endoderm, and ectoderm genes were significantly increased in L-ESCs compared
278 with 2i/L-ESCs (Fig. 6A). Compared with 3-day differentiation, 6-day culturing significantly
279 increased mesoderm, endoderm, and ectoderm genes expression level in 2i/L-ESCs but not in
280 L-ESCs (*SI Appendix*, Fig. S5A and B). This indicates that L-ESCs have strong flexibility and
281 differentiation ability depends on the environment changes. Nevertheless, 6-day
282 differentiation ability between 2i/L-ESCs and L-ESCs was not significantly different (*SI*
283 *Appendix*, Fig. S5C). Furthermore, we confirm protein levels of mesoderm, endoderm and
284 ectoderm markers by immunostaining (Fig. 6B). In addition, similar to 2i/L-ESCs, L-ESCs
285 also generated teratomas that contained derivatives of the three germ layers (Fig. 6C). The
286 results showed that L-ESCs have differentiation ability both *in vitro* and *in vivo*, and is able to
287 express important differentiation genes in a shorter space of time when compared to
288 2i/L-ESCs.

289

290 **Contribution of L-ESCs to full-term embryonic development**

291 Finally, we tested the *in vivo* developmental potential of L-ESCs in chimeric embryos. Using
292 L-ESCs derived from 2i/L-ESCs, we injected L-ESCs into 8-cell stage embryos (Fig. 7A). We
293 noticed that L-ESCs successfully integrated into E13.5 germlines of chimeras. Notably, 36.8%
294 (7/19) of recovered embryos showed chimeric contribution and 57.1% (4/7) of chimeric
295 embryos displayed germlines contribution (Fig. 7B and C). We further tested whether it is
296 possible to obtain L-ESCs-derived postnatal chimeric mice. Of all 20 born pups, 5
297 L-ESCs-derived chimeras (25%) were obtained (Fig. 7D and E). Hence, these data
298 demonstrate the pluripotency of L-ESCs and their chimeric competency to both germlines

299 contribution and full-term development.

300

301 **Discussion**

302 ESCs are derived from the inner cell mass (ICM) of the blastocyst, and self-renew indefinitely
303 *in vitro* (4, 6). The signaling of WNT, ERK and JAK/STAT3 are main regulators that combine
304 to control pluripotency, however, precise function of the individual signaling pathways is
305 unclear (7). In this study, we represent the induction of one novel cell type, L-ESCs from
306 2i/L-ESCs, which depend on JAK/STAT3 signaling alone, and provide new insights on the
307 nature of pluripotent stem cells. In particular, the L-ESCs show higher DNA methylation
308 levels than 2i/L-ESCs (Fig. 3A), and based on transcriptional level, L-ESCs appeared to be at
309 an intermediate state between naïve ESCs and primed EpiSCs (Fig. 2A). We also find that
310 genomic imprints are more stable in L-ESCs relative to 2i/L-ESCs (Fig. 3D). Based on the
311 gene expression and DNA methylome analysis, L-ESCs appeared to be at an intermediate
312 state between naïve ESCs and primed EpiSCs, and may represent stable cells with the
313 characteristics of the early postimplantation epiblast.

314

315 LIF signaling include JAK/STAT, MARK and PI(3)K pathways, and stimulates a states of
316 self-renewal, and determines the fate of cells (7). In mouse ESCs, it is generally believed that
317 LIF signaling is skewed towards survival and self-renewal, whereas activation of canonical
318 WNT signaling and blockade of FGF/ERK blocks cell differentiation (7). In this study we
319 show that under LIF alone medium, some proportion of surviving ESCs acquires new features.
320 These L-ESCs maintained self-renewal and pluripotency over passage 40. We show that

321 L-ESCs died in 10 days in medium with JAK inhibitor (Fig. 1F and G). It has been clear that
322 LIF is critical to L-ESCs self-renewal and to maintain undifferentiated state. One hypothesis
323 is that 2i/L-ESCs cultured in L-medium became heterogeneous, majority of 2i/L-ESCs
324 differentiation in this regime, and only small proportion indicates the presence of naïve ESCs,
325 which the JAK/STAT3 may favor to bind to cofactors or intrinsic factor that promote
326 self-renew. Recently Ying et al reported STAT3 signaling functions in a binary “on/off”
327 manner, however they used S/L medium, the defined mechanism needs to be further explored
328 (36).

329
330 DNA methylation is of paramount importance for mammalian embryonic development and
331 DNA methylation deficient embryos die at such an early stage of development (37). Here, we
332 show that DNA hypermethylation increased the efficiency of L-ESCs reprogramming in S/L
333 medium, whereas *Dnmt3a* and *Dnmt3l* knockout model and 5-Aza treatment affect the
334 efficiency of inducing L-ESCs reprogramming and self-renewal. Interestingly, triple-knockout
335 (TKO) mouse S/L-ESCs for *Dnmt1*, *Dnmt3a* and *Dnmt3b* exhibit DNA hypomethylation,
336 grows robustly and maintains their undifferentiated characteristics (38). Unlike mouse ESCs,
337 conventional ‘primed’ human ESCs cannot tolerate *Dnmt1* deletion, emphasizing the
338 functional differences between mouse and human ESCs (39). We suggest that embryonic stem
339 cells cultured in LIF alone exhibit media dependent DNA hypermethylation and this state
340 support L-ESCs self-renew and proliferation. Notably, LIF-dependent ESCs reprogramming
341 efficiency is significantly reduced in *Dnmt3a* or *Dnmt3l* knockout ESCs (Fig. 7F). We also
342 show that DNMT3A and H3K36me3 expression were higher in L-ESCs compare to

343 2i/L-ESCs. Recently, multiple studies suggested that H3K36me3 participates in cross-talk
344 with other chromatin marks, and promotes de novo DNA methylation by interacting with
345 DNMTs and SETD2 (31). H3K36me3 is responsible for establishing and safeguarding the
346 maternal epigenome (31). Our result showed that H3K36me3 and DNMT3A were highly
347 expressed in L-ESCs, supports this hypothesis.

348

349 Epigenetics including genomic imprinting has widespread roles in mammals, affecting
350 embryonic and placental development and transmission of nutrients to the fetus, and
351 regulating critical aspects of mammalian physiology, such as metabolism, neuronal
352 development and adult behavior (28). We show that L-ESCs reserve hypermethylated
353 imprinting genes, easily differentiate in medium without LIF, which may suggest unique
354 features for ESCs pluripotency. On the other hand, unlike ASCs with high development
355 potency in chimeras, a single L-ESCs do not contribute to development of the embryo to such
356 an extent, suggesting that L-ESCs state is an intermediate between naïve ESCs and primed
357 EpiSCs, and its pluripotency are more close to S/L-ESCs and EpiSCs. In conclusion, this
358 study demonstrates LIF alone is capable to support mouse ESCs reprogramming and provides
359 mechanistic insight into the role of global DNA (de)methylation.

360

361 **Materials and Methods**

362 **Ethics statement**

363 Animal care and use were conducted in accordance with the guidelines of Inner Mongolia
364 University, China. Mice were housed in a temperature-controlled room with proper

365 darkness-light cycles, fed with a regular diet, and maintained under the care of the Laboratory
366 Animal Unit, Inner Mongolia University, China. The mice were sacrificed by cervical
367 dislocation. This study was specifically approved by the Institutional Animal Care and Use
368 Committee, Inner Mongolia University, China. Oct4- Δ PE-GFP (GOF/GFP) transgenic mice
369 (19) were used here with a mixed background of MF1, 129/sv, and C57BL/6J strains.

370

371 **Derivation of 2i/L-ESCs**

372 Mouse embryos blastocysts (E3.5) were isolated from 129/sv females mated with GOF/GFP
373 transgenic males. Green fluorescence indicated that GFP expression of the reporter is under
374 the control of *Oct4* promoter and distal enhancer. This GFP transgene shows expression in the
375 ICM of blastocysts and PGC *in vivo*, and in ESCs (19). ESCs culture medium consists of
376 N2B27 medium (Life technology) supplemented with PD0325901 (PD, 1 μ M, Miltenyi
377 Biotec), CHIR99021 (CH, 3 μ M, Miltenyi Biotec) and leukemia inhibitory factor (LIF, 1000
378 IU/ml, Millipore), henceforth were called 2i/L medium. Zona pellucida of blastocysts were
379 removed by Acidic Tyrode's Solution (Sigma-Aldrich), and then placed to 24-well
380 fibronectin-coated (FN, 16.7 μ g/ml, Millipore) plate with 2i/L medium. ICM of blastocysts
381 cultures grew efficiently and formed outgrowing colonies in 5-7 days culture. The resulting
382 colonies were further cutting into smaller pieces by glass needles after 5-7 days culture, and
383 then the colonies passaged by Accutase (Life technology) regularly on at every 2 days
384 interval.

385

386

387 **Derivation of L-ESCs**

388 1×10^5 2i/L-ESCs were switched on fibronectin-coated (16.7 $\mu\text{g/ml}$, Millipore) 24-well cell
389 culture plate containing L-medium which are N2B27 medium supplemented with leukemia
390 inhibitory factor (1000 IU/ml, Millipore), and we call these cells as L-ESCs. Dependent on
391 cell growth, L-ESCs were passage every other day in the early stage. After being cultured for
392 4-5 passages or 14-42 passages, GOF/GFP positive and negative L-ESCs were purified by
393 flow-cytometry sorting by BD FACSAria (BD Biosciences) and further analysis. GOF/GFP
394 positive purified L-ESCs were passage every other day treated with Accutase (Life
395 technology). L-ESCs were capable of self-renewal for over 40 passages. For inhibitor
396 treatment experiment, we added JAK inhibitor I (0.6 μM , Calbiochem) or 5-Aza (6 μM ,
397 Sigma) into L-ESCs culture medium.

398

399 **Derivation of S/L-ESCs**

400 2i/L-ESCs were switch to fibronectin-coated plate with standard ES medium (Knockout
401 DMEM; Knockout Dulbecco's modified Eagle's medium) supplemented with 20% fetal calf
402 serum, 0.1 mM 2-mercaptoethanol, 2 mM L-glutamine, 0.1 mM non-essential amino acid, 50
403 U/ml Penicillin/Streptomycin and 1000U/ml LIF without feeder cells, we named these cells as
404 S/L-ESCs.

405

406 **Cell differentiation**

407 2i/L-ESCs and L-ESCs were cultured in N2B27 medium for 3 to 6 days withdrawal of
408 PD0325901, CHIR99021 and LIF, and LIF respectively.

409 **Colony formation assay**

410 Single 2i/L-ESCs and L-ESCs were seeded at a fibronectin-coated 96-well plates using mouth
411 pipette, containing 2i/L and L-medium, respectively. The cells were cultured for 10 days and
412 the number of colonies was assessed.

413

414 **Western blot**

415 Cells were collected with Accutase (Life technology), washed three times with DPBS, and
416 lysed in buffer that contained 20 mM Tris (pH 8.0), 137 mM NaCl, 100 g/l glycerol, 50 g/l
417 Triton X-100, and 4 g/l EDTA; 1 µl PMSF (0.1 M) and 10 µl phosphatase inhibitor (10 g/l)
418 were added per 1 ml lysis buffer immediately before use. Proteins were denatured with 2 ×
419 SDS at 95 °C for 5 min. A total of 20 µg denatured protein was run on 8% or 10% SDS–
420 PAGE gel and transferred to polyvinylidene difluoride (PVDF) membrane. Membranes were
421 blocked with 5% nonfat milk in 1 × TBS with 0.05% Tween-20 (TBST) for 1h. Samples were
422 probed with primary antibodies overnight at 4 °C. The primary antibodies used were
423 anti-DNMT3A (CST, 3598S; dilution 1:1,000), anti-H3K36me3 (Abcam, ab9050; working
424 concentration, 1 µg/ml), and anti-β-ACTIN (Abcam, ab8227; dilution 1:5,000). Blots were
425 rinsed with TBST. Membranes were incubated with HRP-conjugated secondary antibodies for
426 60 min at room temperature, and proteins were detected by ECL plus reagent. After rinsing
427 with TBST, ClarityTM Western ECL Substrate (BIO-RAD) was used for visualization, and
428 ChemiDocTM MP Imaging System (BIO-RAD) was used for band detection.

429

430

431 **Alkaline phosphatase (AP) staining**

432 AP staining was carried out using AP staining kit from Sigma (86R-1KT) according to
433 manufacturer's instructions. Briefly, the cells were fixed by 4% paraformaldehyde for 10 min,
434 and then were stained by AP staining solution for overnight at room temperature.

435

436 **Immunostaining**

437 Cultured ESCs were briefly washed with PBS and fixed in 4% paraformaldehyde in PBS for
438 15 min at room temperature. Cells were permeabilized for 30 min with 1% BSA and 0.1%
439 Triton X-100 in PBS. Antibody staining was carried out in the same buffer at 4 °C for
440 overnight. The slides were subsequently washed three times in 1% BSA, 0.1% Triton X-100
441 in PBS (5 min each wash), were incubated with secondary antibody for 1h at room
442 temperature in the dark, washed once for 5 min in 1% BSA, 0.1% Triton X-100 in PBS and
443 twice for 5 min in PBS. The slides were then mounted in Vectashield with DAPI (Vector
444 Laboratories) and imaged using a Olympus FV1000 confocal microscope. Primary antibodies
445 used were: anti-OCT4 (BD Biosciences, Catalog Number: 611203, 1:200), anti-NANOG
446 (eBioscience, Catalog Number: 14-5761, 1:500), anti-SOX2 (Santa cruz, Catalog Number:
447 sc-17320, 1:200), anti-H3K27me3 (Upstate, Catalog Number: 07-449, 1:500), anti-ZSCAN4
448 (Abcam, Catalog Number: ab106646, 1:200), anti-MERVL (HuaAn Bio, Catalog Number:
449 ER50102, 1:100), anti-DNMT3A (abcam, Catalog Number: ab79822, 1:500), anti-NESTIN
450 (BOSTER Bio, Catalog Number: BM4494, 1:50), anti-BRACHYURY (R & D Systems,
451 Catalog Number: AF2085, 1:100) and anti-SOX17 (R & D Systems, Catalog Number:

452 AF1924, 1:100). All secondary antibodies used were Alexa Fluor highly cross adsorbed
453 (Molecular Probes).

454

455 **Flow cytometry**

456 GOF/GFP ESCs were harvested by Accutae and sorting by BD LSRFortessa. Green
457 fluorescence indicated that GFP expression of the reporter is under the control of Oct4
458 promoter and distal enhancer. This GFP transgene shows expression in the ICM of blastocysts
459 and PGCs in vivo, and in ESCs. No GOF/GFP ESCs were used for FACS gating negative
460 control. Measure fluorescence (detector 488 nm channel for GFP) by flow cytometer. Gating
461 out of residual cell debris and measure diploid and tetraploid DNA peaks. A region
462 representing GFP-positive cells were used to identify living cells and collected.

463

464 **Teratomas formation**

465 The 2i/L-ESCs and L-ESCs were disaggregated using Accutase, and 1×10^6 cells were injected
466 into under epithelium of NOD–SCID mice. Three to five weeks after transplantation, tumor(s)
467 were collected and fixed with 4% paraformaldehyde, and processed for paraffin sectioning.
468 Sections were observed following Hematoxylin and Eosin staining.

469

470 **Karyotyping**

471 ESCs were prepared for cytogenetic analysis by treatment with colcemid (Sigma) at a final
472 concentration of 0.1 $\mu\text{g/ml}$ for 3h to accumulate cells in metaphase. Cells were then exposed

473 to 0.075 M KCl for 25 min at 37°C and fixed with 3:1 methanol: acetic acid. Air-dried slides
474 were generated and G-banded following standard GTG banding protocols.

475

476 **Production of chimeras**

477 8-10 ESCs were injected gently into the ICR mice eight-cell stage embryos using a
478 piezo-assisted micromanipulator attached to an inverted microscope. The injected embryos
479 were cultured in KSOM medium (Millipore) at 37 °C in a 5% CO₂ atmosphere for overnight
480 and then transferred to the uteri of pseudopregnant ICR mice at 2.5 days post coitus (dpc).
481 The embryos were isolated at embryonic stage E13.5 and check germline transmission. Full
482 term chimeras were confirmed by the coat color pattern of the pups at birth.

483

484 **Real-Time PCR**

485 Total RNA was isolated with the RNeasy Plus Mini Kit (Qiagen) and reverse transcribed into
486 cDNA using the Reverse Transcription System (Promega) according to the manufacturer's
487 instructions. Quantitative real-time PCR (qRT-PCR) was conducted using a LightCycler® 96
488 Instrument (Roche Molecular Systems) and qRT-PCR reaction was performed with KAPA
489 SYBR FAST qPCR kit (KAPA Biosystems). At least triplicate samples were assessed for
490 each gene of interest, and GAPDH was used as a control gene. Relative expression levels
491 were determined by the $2^{-\Delta\Delta Ct}$ method. Primer sequences used are given in Table S2.

492

493 **Generation of *Dnmt3a* knockout ASCs lines**

494 Guide RNA sequences were cloned into the plasmid px459 (Addgene, 62988). px459

495 containing *Dnmt3a* gRNAs were co-transfected into digested single ASC by Lipofectamine
496 2000 (Thermo Fisher Scientific). Single cell derived colonies were picked and expanded
497 individually. Genomic DNA of colonies were extracted using the DNeasy Blood & Tissue Kit,
498 which was further analyzed by genomic PCR. Colonies with the deletion of *Dnmt3a* locus
499 were identified. *Dnmt3a* knockout ASCs (*Dnmt3a*^{-/-} ASCs) were cultured in ABCL medium
500 without puromycin. Guide RNA sequences and genotyping primer sequences used are given
501 in Table S2.

502

503 **RNA extraction and sequencing**

504 Total RNA were extracted from approximately one million to two million cells using RNeasy
505 Mini Kit (QIAGEN) according to the recommendation of manufacturer and then NEBNext®
506 Poly (A) mRNA Magnetic Isolation Module was used to isolate mRNA from total RNA.
507 Using mRNA as input, the first and second strand cDNAs were synthesized by NEBNext®
508 RNA First Strand Synthesis Module and NEBNext® Ultra II Non-Directional RNA Second
509 Strand Synthesis Module, respectively. Final libraries were prepared using KAPA Hyper Prep
510 Kits (8 PCR cycles) and sequenced on HiSeq4000 platform.

511

512 **RNA-seq data analysis**

513 Before alignment, raw data were first trimmed to remove reads with more than 10% low
514 quality bases and to trim adaptors. Then the clean reads were mapped to mouse reference
515 genome (mm10) with Tophat (2.0.12) with default settings (40). HTSeq (0.6.1) was used to do
516 the reads counting, and then RefSeq gene expression level was estimated by RPKM method

517 (Reads per kilobase transcriptome per million reads). Data of RNA-seq of S/L-ESCs and
518 EpiSCs (GSE119985) were downloaded from previous study. Differentially expressed genes
519 (DEGs) in different samples were determined by edgeR package with fold-change ≥ 2 and
520 p value ≤ 0.5 (41). Unsupervised hierarchical clustering (UHC) analysis was performed by
521 the R hclust function. Heatmaps of select genes were performed using R heatmap.2 function.
522 Principal component analysis (PCA) analysis was performed with the R prcomp function.
523 Gene ontology analysis was performed using Metascape (<http://metascape.org>). Trend
524 analysis of DEGs was performed using Short Time-series Expression Miner (STEM) software
525 (24).

526

527 **Genomic DNA isolation and WGBS library preparation**

528 Following the manufacturer's instructions, genomic DNA was extracted from stem cells using
529 the DNeasy Blood & Tissue Kit (Qiagen). Remaining RNA was removed by treating with
530 RNase A. Three replicated samples from each of these stem cells were used for library
531 preparation to ensure repeatability of experiment. In short, 2 μg of genomic DNA spiked with
532 10 ng of lambda DNA were fragmented to about 300 bp with Covaris S220. Next, end repair
533 and A-ligation were performed to the DNA fragments. Methylated Adaptor (NEB) was then
534 ligated to the DNA fragments. In order to reach >99% bisulfite conversion, the adaptor-ligated
535 DNA was treated twice using EZ-96 DNA Methylation-Direct™ MagPrep (Zymo Research).
536 The resulting single-strand DNA fragments were amplified by 4 PCR cycles using the KAPA
537 HiFi HotStart Uracil+ ReadyMix (2 \times). At last, the libraries were sequenced on HiSeq4000
538 platform to generate 150-bp paired-end reads.

539 **DNA methylation analysis**

540 Whole genome bisulfite sequencing reads were trimmed with Trim Galore (v0.3.3) to remove
541 adaptors and low quality bases. Then we used Bismark (v0.7.6) (42) to map the clean reads to
542 mouse reference genome (mm10) with a paired-end and non-directional model, then the
543 unmapped reads were realigned to the same genome with a single-end and non-directional
544 model. PCR duplications were removed with command ‘samtools rmdup’ (v0.1.18). WGBS
545 data of 2i/L-ESCs and S/L-ESCs were downloaded from previous study (GSE98517) (8) and
546 identically processed. The global DNA methylation level, estimated using a 2 kb window
547 across the genome, and DNA methylation level in each genomic regions was estimated based
548 on 3x CpG sites (CpGs covered more than 3 times). Only regions with more than 3 CpGs
549 covered were retained. Genomic annotation, like exons, introns and repeat regions were
550 downloaded from UCSC genome browser. Promoters were regions 1 kb upstream and 0.5 kb
551 downstream of transcription start sites (TSS). Imprint control regions (ICR) were obtained
552 from previous study (43), for the low coverage of published S/L-ESCs data, DNA
553 methylation level on ICRs were estimated based on 1x CpG sites. Locations of ICRs were
554 converted with UCSC LiftOver from mm9 to mm10.

555

556 **Data availability**

557 These RNA-seq data are available through the NCBI Sequence Read Archive (SRA) under
558 the ID PRJNA601004
559 (<https://dataview.ncbi.nlm.nih.gov/object/PRJNA601004?reviewer=ckal7bagkptogce20v1qf6>
560 [mp2o](#)). WGBS data have been deposited in the NCBI Gene expression omnibus (GEO) under

583 **Competing interests**

584 The authors declare no competing interest.

585

586 **References**

- 587 1. M. J. Evans, M. H. Kaufman, Establishment in culture of pluripotential cells from mouse embryos.
588 *Nature* **292**, 154-156 (1981).
- 589 2. G. R. Martin, Isolation of a pluripotent cell line from early mouse embryos cultured in medium
590 conditioned by teratocarcinoma stem cells. *Proceedings of the National Academy of Sciences of the*
591 *United States of America* **78**, 7634-7638 (1981).
- 592 3. A. G. Smith *et al.*, Inhibition of pluripotential embryonic stem cell differentiation by purified
593 polypeptides. *Nature* **336**, 688-690 (1988).
- 594 4. Q. L. Ying, J. Nichols, I. Chambers, A. Smith, BMP induction of Id proteins suppresses differentiation
595 and sustains embryonic stem cell self-renewal in collaboration with STAT3. *Cell* **115**, 281-292 (2003).
- 596 5. R. L. Williams *et al.*, Myeloid leukaemia inhibitory factor maintains the developmental potential of
597 embryonic stem cells. *Nature* **336**, 684-687 (1988).
- 598 6. Q. L. Ying *et al.*, The ground state of embryonic stem cell self-renewal. *Nature* **453**, 519-523 (2008).
- 599 7. S. Ohtsuka, Y. Nakai-Futatsugi, H. Niwa, LIF signal in mouse embryonic stem cells. *Jak-Stat* **4**,
600 e1086520 (2015).
- 601 8. J. A. Hackett, T. Kobayashi, S. Dietmann, M. A. Surani, Activation of Lineage Regulators and
602 Transposable Elements across a Pluripotent Spectrum. *Stem cell reports* **8**, 1645-1658 (2017).
- 603 9. A. G. Smith, Embryo-derived stem cells: of mice and men. *Annual review of cell and developmental*
604 *biology* **17**, 435-462 (2001).
- 605 10. J. Yang *et al.*, Establishment of mouse expanded potential stem cells. *Nature* **550**, 393-397 (2017).
- 606 11. Y. Yang *et al.*, Derivation of Pluripotent Stem Cells with In Vivo Embryonic and Extraembryonic
607 Potency. *Cell* **169**, 243-257 e225 (2017).
- 608 12. X. Gao *et al.*, Establishment of porcine and human expanded potential stem cells. *Nature cell biology*
609 **21**, 687-699 (2019).
- 610 13. H. G. Leitch *et al.*, Naive pluripotency is associated with global DNA hypomethylation. *Nature*
611 *structural & molecular biology* **20**, 311-316 (2013).
- 612 14. M. B. Stadler *et al.*, DNA-binding factors shape the mouse methylome at distal regulatory regions.
613 *Nature* **480**, 490-495 (2011).
- 614 15. M. Yagi *et al.*, Derivation of ground-state female ES cells maintaining gamete-derived DNA
615 methylation. *Nature* **548**, 224-227 (2017).
- 616 16. J. Choi *et al.*, Prolonged Mek1/2 suppression impairs the developmental potential of embryonic stem
617 cells. *Nature* **548**, 219-223 (2017).
- 618 17. S. Bao *et al.*, Derivation of hypermethylated pluripotent embryonic stem cells with high potency. *Cell*
619 *research* **28**, 22-34 (2018).
- 620 18. G. Huang, S. Ye, X. Zhou, D. Liu, Q. L. Ying, Molecular basis of embryonic stem cell self-renewal:
621 from signaling pathways to pluripotency network. *Cellular and molecular life sciences : CMLS* **72**,
622 1741-1757 (2015).

- 623 19. T. Yoshimizu *et al.*, Germline-specific expression of the Oct-4/green fluorescent protein (GFP)
624 transgene in mice. *Development, growth & differentiation* **41**, 675-684 (1999).
- 625 20. M. Li, J. C. Izpisua Belmonte, Deconstructing the pluripotency gene regulatory network. *Nature cell*
626 *biology* **20**, 382-392 (2018).
- 627 21. T. S. Macfarlan *et al.*, Embryonic stem cell potency fluctuates with endogenous retrovirus activity.
628 *Nature* **487**, 57-63 (2012).
- 629 22. V. Pasque *et al.*, X Chromosome Dosage Influences DNA Methylation Dynamics during
630 Reprogramming to Mouse iPSCs. *Stem cell reports* **10**, 1537-1550 (2018).
- 631 23. E. G. Schulz *et al.*, The two active X chromosomes in female ESCs block exit from the pluripotent state
632 by modulating the ESC signaling network. *Cell stem cell* **14**, 203-216 (2014).
- 633 24. J. Ernst, Z. Bar-Joseph, STEM: a tool for the analysis of short time series gene expression data. *BMC*
634 *bioinformatics* **7**, 191 (2006).
- 635 25. E. Habibi *et al.*, Whole-genome bisulfite sequencing of two distinct interconvertible DNA methylomes
636 of mouse embryonic stem cells. *Cell stem cell* **13**, 360-369 (2013).
- 637 26. O. Joshi *et al.*, Dynamic Reorganization of Extremely Long-Range Promoter-Promoter Interactions
638 between Two States of Pluripotency. *Cell stem cell* **17**, 748-757 (2015).
- 639 27. M. Ter Huurne, J. Chappell, S. Dalton, H. G. Stunnenberg, Distinct Cell-Cycle Control in Two Different
640 States of Mouse Pluripotency. *Cell stem cell* **21**, 449-455 e444 (2017).
- 641 28. R. N. Plasschaert, M. S. Bartolomei, Genomic imprinting in development, growth, behavior and stem
642 cells. *Development* **141**, 1805-1813 (2014).
- 643 29. T. Wu *et al.*, Histone variant H2A.X deposition pattern serves as a functional epigenetic mark for
644 distinguishing the developmental potentials of iPSCs. *Cell stem cell* **15**, 281-294 (2014).
- 645 30. B. Wu *et al.*, Activin A and BMP4 Signaling Expands Potency of Mouse Embryonic Stem Cells in
646 Serum-Free Media. *Stem cell reports* **14**, 241-255 (2020).
- 647 31. Q. Xu *et al.*, SETD2 regulates the maternal epigenome, genomic imprinting and embryonic
648 development. *Nature genetics* **51**, 844-856 (2019).
- 649 32. M. J. Beyrouthy *et al.*, High DNA methyltransferase 3B expression mediates 5-aza-deoxycytidine
650 hypersensitivity in testicular germ cell tumors. *Cancer research* **69**, 9360-9366 (2009).
- 651 33. R. Juttermann, E. Li, R. Jaenisch, Toxicity of 5-aza-2'-deoxycytidine to mammalian cells is mediated
652 primarily by covalent trapping of DNA methyltransferase rather than DNA demethylation. *Proceedings*
653 *of the National Academy of Sciences of the United States of America* **91**, 11797-11801 (1994).
- 654 34. A. De Los Angeles *et al.*, Hallmarks of pluripotency. *Nature* **525**, 469-478 (2015).
- 655 35. X. Shen *et al.*, EZH1 mediates methylation on histone H3 lysine 27 and complements EZH2 in
656 maintaining stem cell identity and executing pluripotency. *Molecular cell* **32**, 491-502 (2008).
- 657 36. C. I. Tai, E. N. Schulze, Q. L. Ying, Stat3 signaling regulates embryonic stem cell fate in a
658 dose-dependent manner. *Biology open* **3**, 958-965 (2014).
- 659 37. M. V. C. Greenberg, D. Bourc'his, The diverse roles of DNA methylation in mammalian development
660 and disease. *Nature reviews. Molecular cell biology* **20**, 590-607 (2019).
- 661 38. A. Tsumura *et al.*, Maintenance of self-renewal ability of mouse embryonic stem cells in the absence of
662 DNA methyltransferases Dnmt1, Dnmt3a and Dnmt3b. *Genes to cells : devoted to molecular & cellular*
663 *mechanisms* **11**, 805-814 (2006).
- 664 39. J. Liao *et al.*, Targeted disruption of DNMT1, DNMT3A and DNMT3B in human embryonic stem cells.
665 *Nature genetics* **47**, 469-478 (2015).
- 666 40. C. Trapnell, L. Pachter, S. L. Salzberg, TopHat: discovering splice junctions with RNA-Seq.

- 667 *Bioinformatics* **25**, 1105-1111 (2009).
- 668 41. M. D. Robinson, D. J. McCarthy, G. K. Smyth, edgeR: a Bioconductor package for differential
669 expression analysis of digital gene expression data. *Bioinformatics* **26**, 139-140 (2010).
- 670 42. F. Krueger, S. R. Andrews, Bismark: a flexible aligner and methylation caller for Bisulfite-Seq
671 applications. *Bioinformatics* **27**, 1571-1572 (2011).
- 672 43. W. Xie *et al.*, Base-resolution analyses of sequence and parent-of-origin dependent DNA methylation in
673 the mouse genome. *Cell* **148**, 816-831 (2012).

674

675 **Figure legends**

676 **Figure 1. LIF alone supports ESCs self-renew and pluripotency.** (A) Experimental outline
677 of the L-ESCs derivation procedures from ESCs. (B) 2i/L-ESCs were switched to L-medium
678 and cultured to passages 3 (p3), p5, p25. Here we use 2i/L-ESCs with GOF/GFP reporter.
679 Scale bars, 100 μm . (C) Karyotyping of L-ESCs (p30). (D) Immunostaining of OCT4, SOX2
680 and NANOG in L-ESCs. Scale bars, 50 μm . (E) Single cell clonogenicity efficiency in
681 L-ESCs and 2i/L-ESCs. (F) L-ESCs were treated with JAK inhibitor I after day 3 p2 and day
682 10 p4. Scale bars, 100 μm . (G) 2i/L-ESCs were treated with JAK inhibitor I after day 3 p2,
683 day 10 p6 and p10. Scale bars, 100 μm .

684 **Figure 2. Analyses of molecular features of L-ESCs.** (A) Unsupervised hierarchical
685 clustering (UHC) of the transcriptome from three biological replicates of four pluripotent
686 stem cell lines. (B) PCA analysis of gene expression of four pluripotent stem cells. (C)
687 Heatmap showing differentially expressed genes (mean $\log_2(\text{normalized read counts}) > 2$,
688 $\log_2(\text{fold change}) > 2$, adjusted $p\text{-value} < 0.05$) in L-ESCs compared with 2i/L-ESCs.
689 Significantly enriched GO terms and representative genes in each cluster are listed on the
690 right. (D) Compared with L-ESCs, 2i/L-ESCs, S/L-ESCs and EpiSCs, among differentially
691 expressed genes, a total of 3,347 genes (profile 7) were significantly high expressed in
692 L-ESCs and 2i/L-ESCs compared with S/L-ESCs and EpiSCs; a total of 1,621 genes (profile

693 2) were significantly upregulated in 2i/L-ESCs, compared with L-ESCs, S/L-ESCs and
694 EpiSCs.

695 **Figure 3. DNA methylation pattern of L-ESCs.** (A) DNA methylation level of 2 kilobase
696 (kb) genomic tiles. Source data are provided in Table S1. (B) Immunostaining of Dnmt3a in
697 2i/L-ESCs and different passages L-ESCs. Scale bars, 50 μ m. (C) Western blotting analysis
698 for Dnmt3a in early reprogramming stage (day 5) L-ESCs (GOF/GFP positive and negative
699 cells). (D) Heatmap showing DNA methylation level of ICRs in three different stem cells.

700 **Figure 4. Serum improves the efficiency of L-ESCs reprogramming.** (A) Left: Alkaline
701 phosphatase (AP) staining on 2i/L-ESCs and S/L-ESCs (2i/L-ESCs were cultured in S/L
702 medium for 5 days) were switched to L-medium and after 10 days culture. Right:
703 Quantification of number of AP positive colonies after 10 days culture. Error bars are mean \pm
704 SD (n = 5). *P* values were calculated by two tailed Student's *t*-test, *p* < 0.05. (B) Left:
705 GOF/GFP positive colonies on 2i/L-ESCs and S/L-ESCs (2i/L-ESCs were cultured in S/L
706 medium for 5 days) were switched to L-medium and after 8 days culture. Scale bars, 100 μ m.
707 Right: Quantification of number of GOF/GFP positive colonies after 8 days culture. Error bars
708 are mean \pm SD (n = 4). *P* values were calculated by two tailed Student's *t*-test, *p* < 0.05. (C)
709 Left: Fluorescence-activated cell sorting (FACS) based on GOF/GFP positive cells, after
710 2i/L-ESCs and S/L-ESCs (2i/L-ESCs were cultured in S/L medium for 5 days) were switched
711 to L-medium and after 4 days culture. Right: Quantification of Percentage of GOF/GFP
712 positive cells after 4 days culture. Error bars are mean \pm SD (n = 3). *P* values were calculated
713 by two tailed Student's *t*-test, *p* < 0.05. (D) Western blotting analysis for H3K36me3 in early
714 reprogramming stage (day 5) L-ESCs (GOF/GFP positive and negative cells).

715 **Figure 5. DNA methylation is indispensable for L-ESCs self-renew.** (A) 2i/L-ESCs were
716 treated with 5-Aza after 3 and 7 days, 2i/L-ESCs retained typical dome-shaped clonal
717 morphology. Scale bars, 100 μm . (B) L-ESCs were treated with 5-Aza after 3 and 7 days,
718 there was a few GOF/GFP⁺ L-ESCs survived after 7 days 5-Aza treatment and to apoptosis in
719 final. Scale bars, 100 μm . (C) Left: AP staining on wild type ESCs and *Dnmt3l*^{-/-} ESCs were
720 switched to L-medium and after 8 days culture. Right: Quantification of number of AP
721 positive colonies after 8 days culture. Error bars are mean \pm SD (n = 8). *P* values were
722 calculated by two tailed Student's *t*-test, *p* < 0.05. (D) Relative expression of *Dnmt3a* by
723 qPCR in *Dnmt3a*^{-/-} ASCs and *Dnmt3a*^{+/+} ASCs. Error bars are mean \pm SD (n = 3). *P* values
724 were calculated by two tailed Student's *t*-test, *p* < 0.05. (E) Western blotting analysis for
725 DNMT3A in *Dnmt3a*^{-/-}-ASCs and *Dnmt3a*^{+/+}-ASCs. (F) Left: GOP/GFP positive colonies on
726 wild type ASCs and *Dnmt3a*^{-/-} ASCs were switched to L-medium and after 10 days culture.
727 Right: Quantification of number of GOP/GFP positive colonies after 10 days culture. Error
728 bars are mean \pm SD (n = 8). *P* values were calculated by two tailed Student's *t*-test, *p* < 0.05.

729 **Figure 6. The pluripotency of L-ESCs *in vivo* and *in vitro*.** (A) Relative expression of
730 mesoderm, endoderm and ectoderm genes measured by qPCR, after L-ESCs were 3 days *in*
731 *vitro* differentiation. Error bars are mean \pm SD (n = 3). *P* values were calculated by two tailed
732 Student's *t*-test, *p* < 0.05. (B) Immunostaining of T, SOX17 and NESTIN, after 2i/L-ESCs and
733 L-ESCs were 6 days *in vitro* differentiation. Scale bars, 50 μm . (C) Mature teratomas from
734 L-ESCs. Left: mesoderm, muscle like cells; middle: endoderm, gland like cells; right:
735 ectoderm, epidermis like cells. The sections were stained with haematoxylineosin. Scale bars,
736 50 μm .

737 **Figure 7. Ability of L-ESCs to full-term embryonic development.** (A) Schematic of eight
738 cell embryos injection protocol. (B) Germline transmission of L-ESCs in E13.5 chimeras.
739 PGCs were shown by GOF/GFP-positive cells (arrow). black arrow: mesonephros; white
740 arrow: gonad; yellow arrow: gonadal PGCs. Scale bars, 100 μ m. (C) Summary of E13.5
741 chimera assays by L-ESCs injection. The black bar chart shows the percentages of chimeras
742 among the collected E13.5 conceptuses, embryonic tissues (Em); gray bar, integration into
743 primordial germ cells (PGCs) among the recovered E13.5 chimeras. (D) Chimeric pups
744 generated by injecting L-ESCs in ICR host blastocysts. (E) The summary of full term
745 chimeric pups were derived by L-ESCs. (F) Schematic of DNA methylation affects LIF
746 dependent embryonic stem cells reprogramming process.

Figure 1

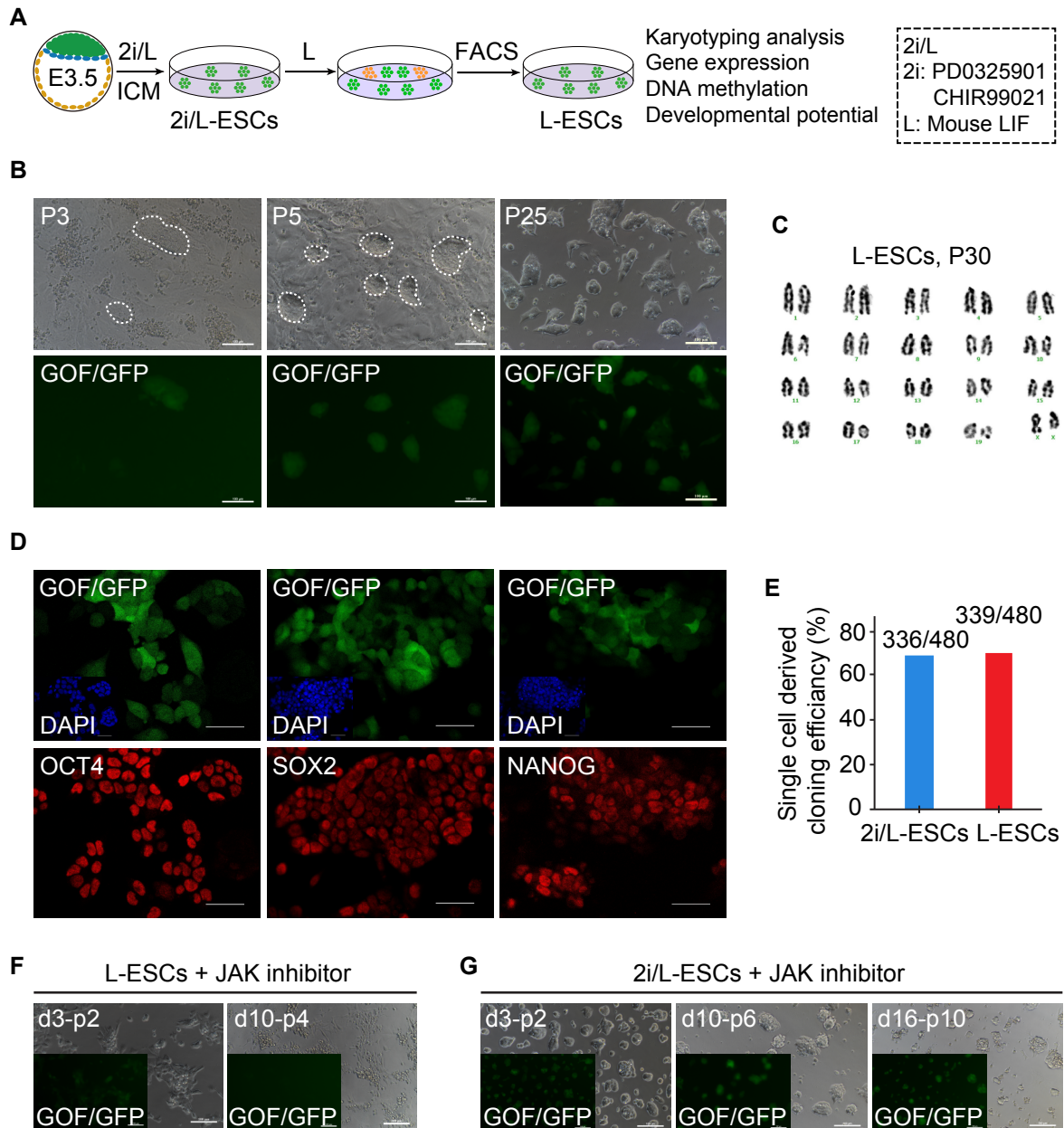


Figure 2

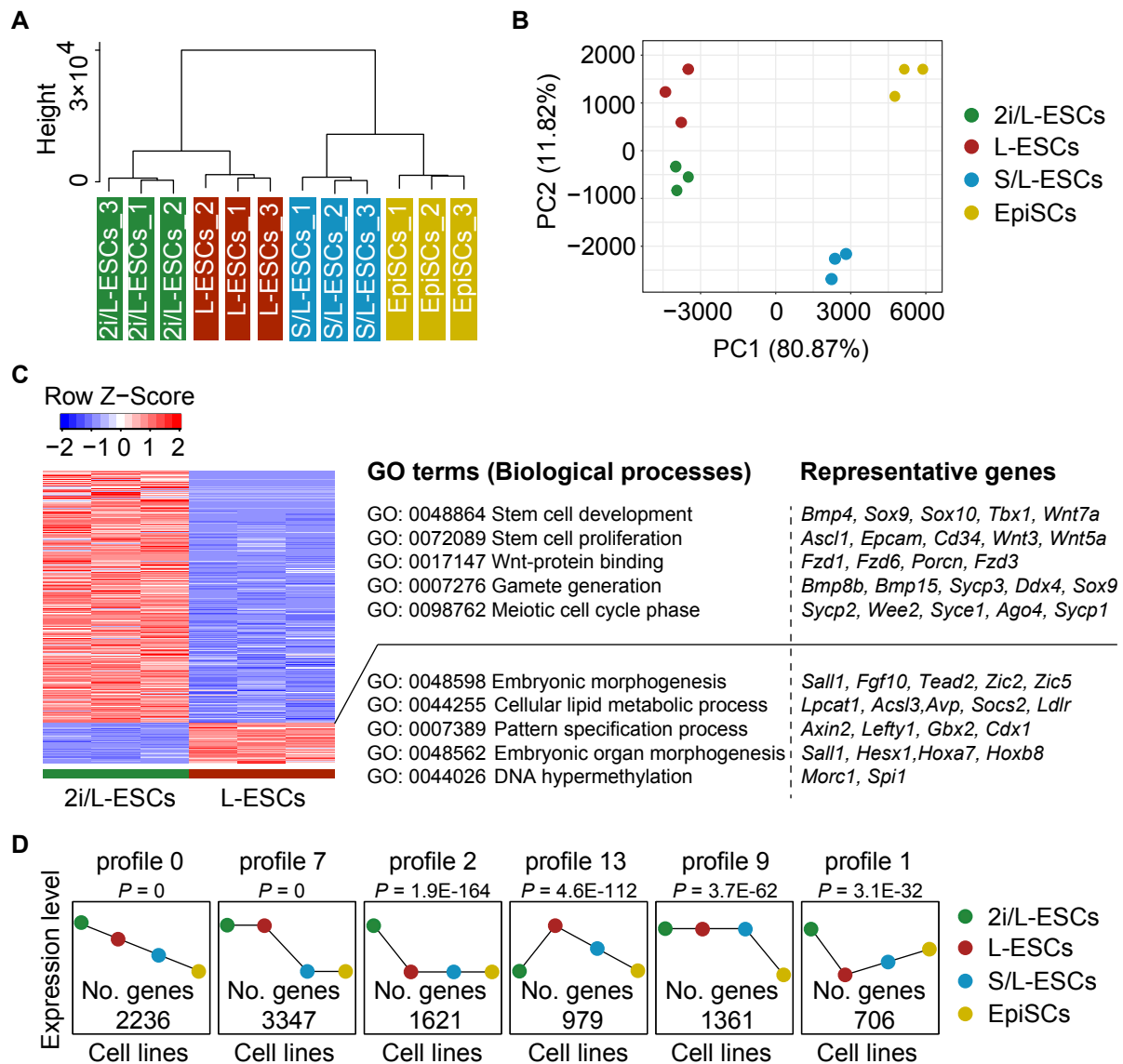


Figure 3

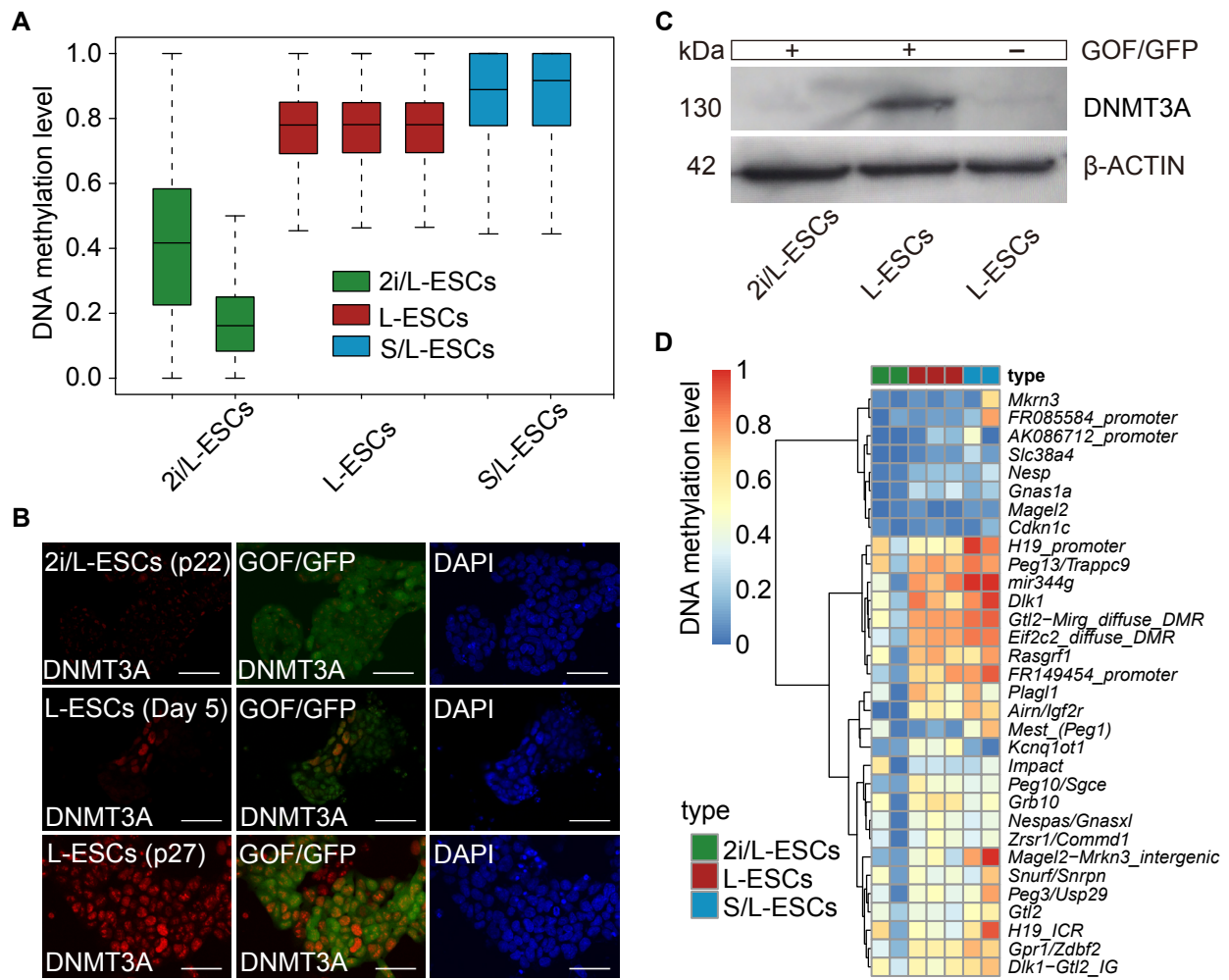


Figure 4

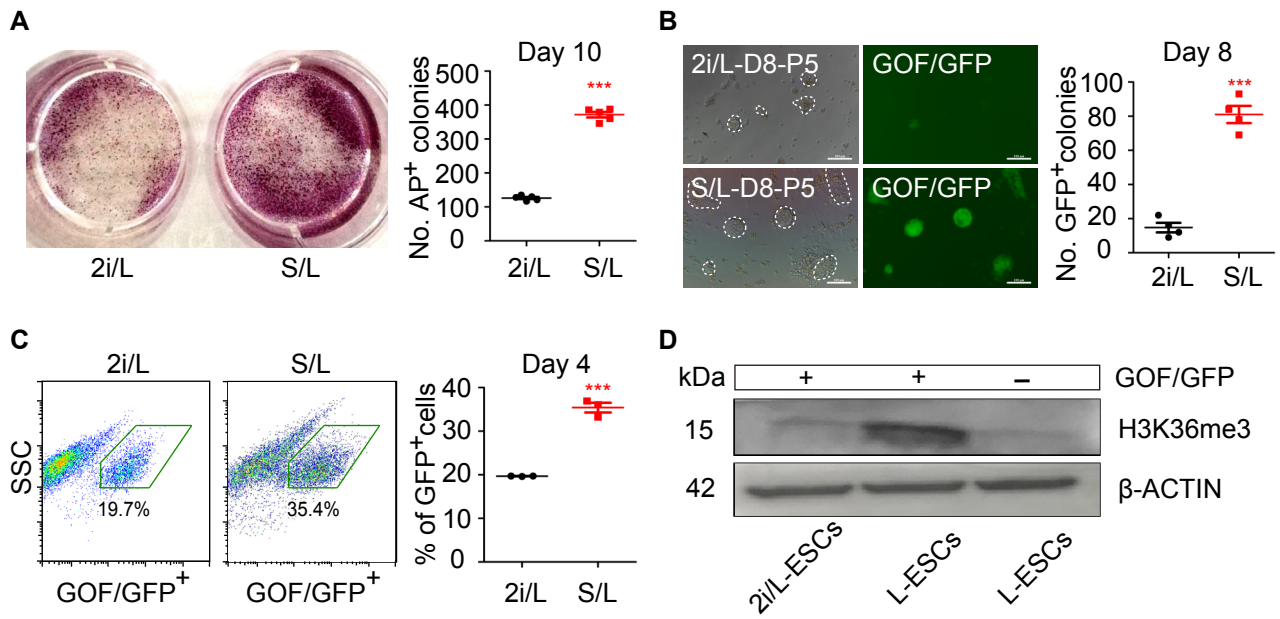


Figure 5

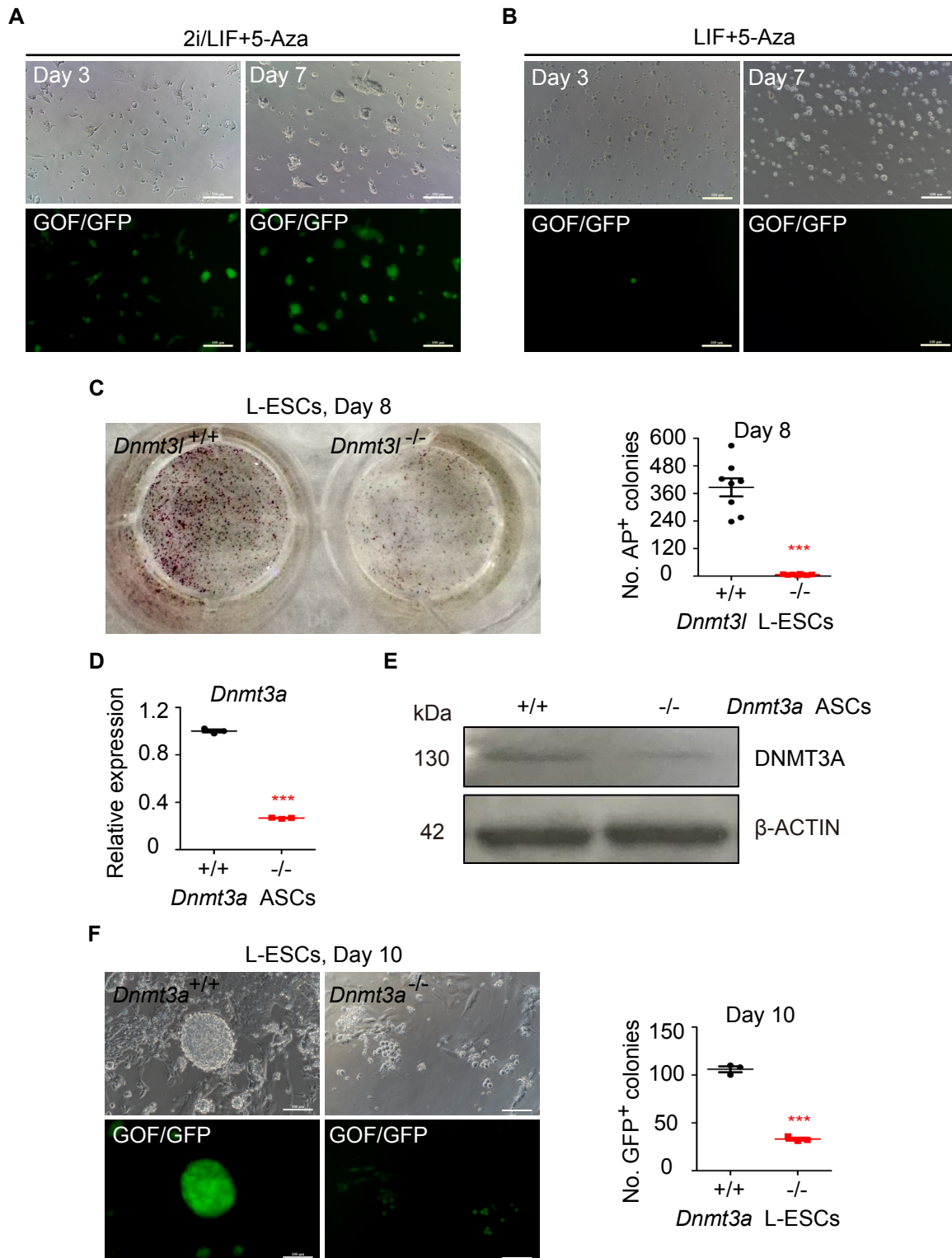


Figure 6

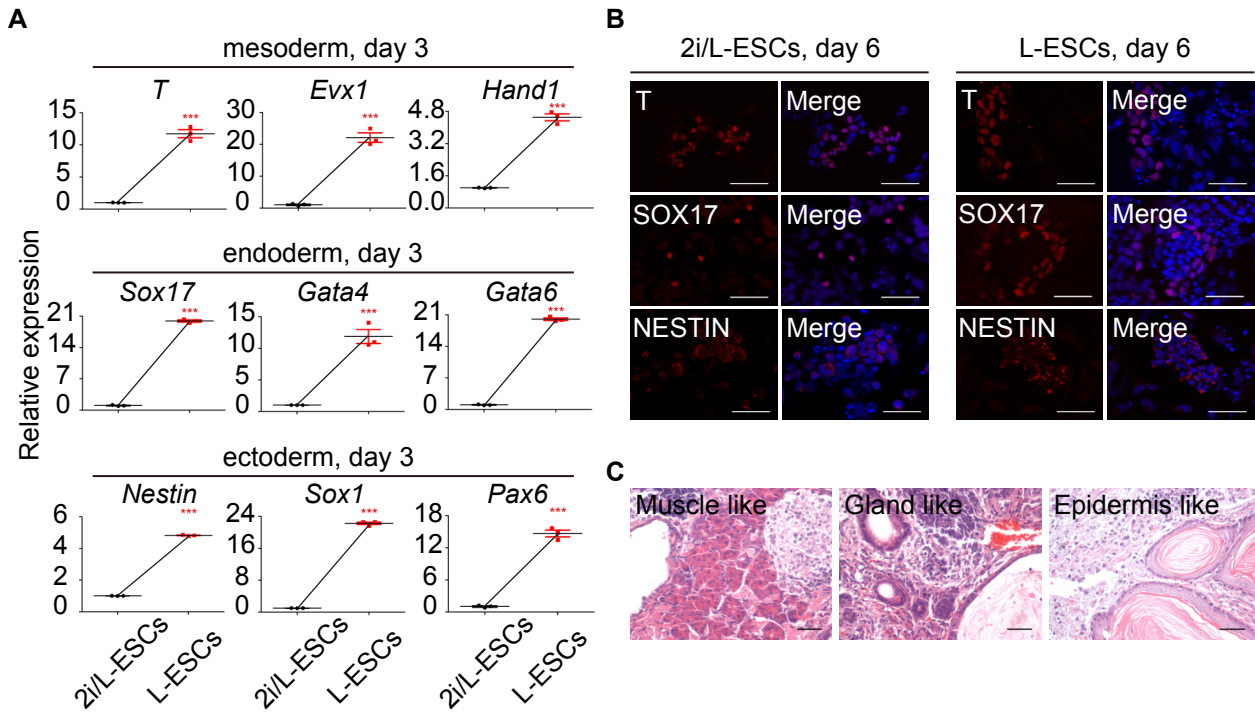


Figure 7

